Comparison of Damage Formation and Crack Propagation Behavior of Selected Nuclear Graphite for HTGR

Se-Hwan Chi [a*], Hyun-Ju Kim, Eung-Seon Kim, Min-Hwan Kim
[a]*Nuclear Hydrogen Development and Demonstration Project, Korea Atomic Energy Research Institute (KAERI), 150 Dukjin-Dong, Yuseong, Daejeon 305-353, Republic of Korea*

[*]*Corresponding author: shchi@kaeri.re.kr*

1. Introduction

HTGR graphite core components are subjected to high energy neutron irradiation during operation resulting in changes to its mechanical and fracture properties. Undoubtedly, these changes are attributed to the irradiation-induced changes in the microstructure of graphite components and finally result in an increase in the probability of fracture of graphite core components menacing the safety of reactor [1, 2].

Due to the nature of HTGR whose core components are made of quasi-brittle graphite, the graphite core components operating for 40-60 years without failure require knowledge and understanding on the characteristics of graphite fracture.

In this study, two results on the fracture of nuclear graphite, i.e., fracture under cyclic compressive loading-unloading and fracture under static loading, were re-evaluated to understand the fracture characteristics of selected nuclear graphite grade for HTGR.

2. Experimental

2.1 Materials and Cyclic Loading-Unloading Test

In this test the crack tip load relaxation behaviors owing to the cyclic compressive loading-unloading (CCLU) of 4-1/3 flexure strength test specimens were investigated based on the load-displacement curves. Three nuclear graphite grades for a high-temperature gas-cooled reactor (HTGR) were chosen based on the manufacturer, forming method, source coke and grain size (coke particle size) (IG-110, NBG-18, PCEA).

Table 1 Graphite grades examined in this study

Grade	Forming method	Source coke	Grain size (average)(㎛)	Density (g/cm^3)
NBG-18	Vibration molding	Pitch	~300	1.85
PCEA	Extrusion	Petroleum	~360	1.87
IG-110	Iso-static molding	Petroleum	~20	1.77

For NBG and PCEA grades, the forming directions during molding or extrusion were considered during the specimen machining from graphite blocks (NBG-18-a, NBG-18-c, PCEA-a, PCEA-c). Specimen size was 16(W) x 18(T) x 64(L) mm with a notch (width: 0.1 mm, length: 7.2 mm, angle: <30±2°). Ten specimens were tested for each grade. Cyclic loading-unloading tests were performed at 0.5 mm/min in compression to 0.13 mm for 10 cycles. The displacement corresponds to 0.81-0.87 of the fracture displacement and 0.65-0.97 of the fracture load for the grades selected.

2.2 Static Fracture Toughness Test

Static fracture toughness test was performed to ASTM D 7779-11 (The Standard Test Method for the Determination of Fracture Toughness of Graphite at Ambient Temperature). The notch of SENB specimens [W(12) x 6.5(T) x 50(L)mm] was machined by EDM. Eight specimens were tested for IG-110, and 16 specimens were tested for PCEA and NBG-18 (8 specimens for each a and c notch direction). The K_{IC} and G-Δa curves were obtained by processing the load and displacement signals using the installed software on Instron Model: 5867 (Labview).

The Critical Stress Intensity Factor, K_{Ic}, was calculated for three-point flexure with $5 \le S/W \le 10$, and $0.35 \le a/W \le 0.60$ using eq. (1):

$$K_{Ic} = g\left[\frac{P_{max} S 10^{-6}}{B W^{3/2}}\right]\left[\frac{3[a/W]^{1/2}}{2[1-a/W]^{3/2}}\right] \quad \text{(eq. 1)}$$

Where:
K_{Ic} = fracture toughness (MPa√m),
g = g(a/W)
= function of the ratio a/W,
P_{max} = maximum force (N),
S = support span (m)
B = breadth (width) of the specimen (m),
W = specimen depth (m), and
a = notch depth (m)

Where:

$g = g(a/W)$

$$g = A_0 + A_1(a/W) + A_2(a/W)^2 + A_3(a/W)^3 + A_4(a/W)^4 + A_5(a/W)^5 \quad \text{(eq. 2)}$$

$C_n = D_n / P_n$

C_n: Compliance for the point n (m/N)
D_n: displacement for the point n (m)
P_n : loading force for the point n (N).

Initial Crack length, a_0 = notch depth
$a_n = a_{n-1} + [(W - a_{n-1})/2 * ((C_n - C_{n-1})/C_{n-1})]$

$G(a_n) = P^2/2B * \delta C/\delta a$ [J/m²],
$\delta C = C_n - C_{n-1}$, $\delta a = a_n - a_{n-1}$

G-Δa, where Δa = $a_n - a_0$

The load-displacement curves were obtained under 0.1 mm/min loading rate (1 KN load cell).

3. Results

3.1. Load Relaxation during the Cyclic Loading-Unloading.

Table 2 shows the results of cyclic loading-unloading test. It is worth noting that the relaxation loads are attributed to the 10 cyclic loading-unloading. As seen, all the grades showed grade dependent cyclic softening behaviors with relatively large anisotropy for NBG and PCEA. Though not large, it is worth noting that an apparent grade dependency is observed between the grades and notch direction (anisotropy).

Table 2. Summary of The Cyclic Load Relaxation (%).

Grade	Initial load before unloading (Kg)	Relaxation load (Kg) for 10 cycles	Relaxation load (%)
IG-110	59.2	0.7	1.18
NBG-18 (a)	75.3	0.3	0.40
NBG-18 (c)	78.8	0.9	1.14
PCEA (a)	75.8	0.2	0.26
PCEA (c)	70.4	0.9	1.28

3.2. Fracture Parameters(K_{IC}, G_{IC}) and G-Δa Behavior.

Table 3 summarizes the results of fracture toughness testing. It is seen that both the local (K_{IC}) and global (G) fracture properties of the PCEA and NBG-18 are better than the IG-110, and the difference is far apparent in G than the K_{IC} parameter.

Table 3. Summary of Fracture Toughness Test: K_{IC}(a), G_{IC} and G fracture parameters (b).

		IG-110	NBG-18-a	NBG-18-c	PCEA-a	PCEA-c
K_{IC} [MPa $(m)^{1/2}$]	6.5 T	0.78 ± 0.02	1.10 ± 0.07	1.04 ±0.13	1.15 ±0.02	1.07 ±0.04

(a)

		IG-110	NBG-18-a	NBG-18-c	PCEA-a	PCEA-c
G_{IC} [J/m^2],	6.5T	200	800	560	750	670
SCL (%)	6.5T	32.0	47.0	40.0	46.0	45.0
ΔG (%)	6.5T	225 (112)	1400 (175)	878 (157)	1775 (237)	1455 (217)
$(\Delta G_{B-A}/\Delta a_{B-A})$ J/m3	6.5T	180.0	773.5	566.5	980.7	?

(b)

3.3 Correlation between the Relaxation load and Fracture Parameters.

Fig. 1 shows the correlations between the load relaxation (%) and fracture parameters (K_{IC}, G_{IC}, ΔG, ΔG/Δa).

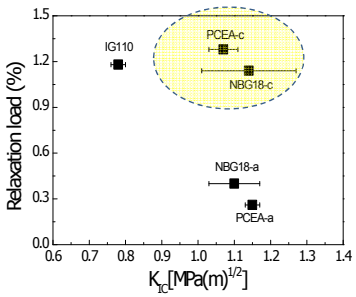

(a)

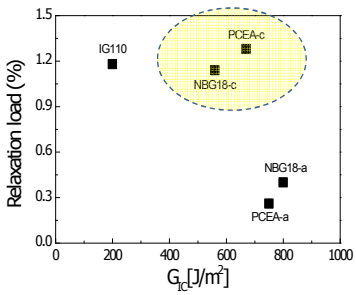

(b)

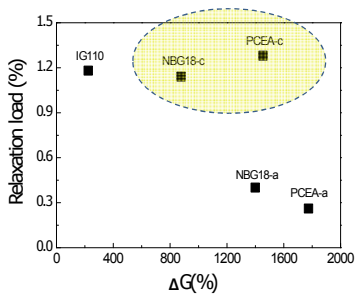

(c)

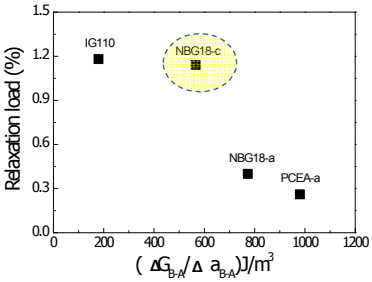

(d)

Fig. 1. Correlation between the relaxation load (from cyclic loading-unloading test) and fracture parameters (from fracture toughness test): (a) K_{IC} (b) G_{IC} (c) ΔG (d) $\Delta G/\Delta a$.

Fig. 1 shows that, if the data from NBG-18-c and PCEA-c are excluded (data encircled), over all, the higher the relaxation load, the lower the fracture characteristics related to the resistance of the grades to crack initiation (Fig. 1. (1) and (2)) and propagation (Fig. 1. (c) and (d)).
Apparent differences in the fracture parameters owing to the anisotropy are noted for the NBG and PCEA grades. A weak anisotropy as observed in the fracture parameters to the relaxation load may reflect the progress of forming technology development (NBG-18 and PCEA).

4. Discussion

In view from the differences in microstructure and forming methods of the grades, the grade of fine grain and isotropic molding appears to form fracture process zone (FPZ) with lower energy consumption than the grades of medium grain and extrusion or vibration molding. Then, the lower energy consumption during the damage formation and stable crack growth stage in the FPZ should result in a larger load relaxation with a larger FPZ volume and an increased fine crack accumulation [3, 4]. All these changes in the FPZ of the fine grain and isotropic molded grade will lead to a lower resistance to crack formation and initiation (Lower K_{IC}) and finally crack extension (lower ΔG and $\Delta G/\Delta a$).

A weak anisotropy as observed in the fracture parameters to the relaxation load may reflect the progress of forming technology development (NBG-18 and PCEA). It is of noted that the small differences in load relaxation are correlated well with the fracture toughness parameters.

5. Conclusion

Present observation may need to be considered in the graphite selection as well as in the design and safety evaluation of the graphite core components in HTGR.

REFERENCES

[1] T. D. Burchell, Fission Reactor Application of Carbon, Chapter 13 in Carbon Materials for Advanced Technologies, Pergamon, London, pp. 429-478, 1999.
[2] Se-Hwan Chi, Chapter. 6.1.3.2 Radiation Damage in Introduction to High Temperature Gas-Cooled Reactor Engineering (Ed. Jonghwa Chang), KAERI/GP-362/2014, pp. 342-364, 2014 (in Korean).
[3] T. H. Becker, T. J. Marrow, R. B. Tait, Damage, Crack growth and fracture characteristics of nuclear grade graphite using the Double Torsion technique, Journal of nuclear materials, Vol. 414, pp. 32-43, 2011.
[4] R. K. L. Su, H. H. Chen, S. L. Fok, H. Li, G. Sing, L. Sun. L. Shi, Determination of the tension softening curve of nuclear graphite using the incremental displacement collocation method, Carbon, Vol. 57, pp. 65-78, 2013.